

# Tailoring the particle size from $\mu\text{m}$ $\rightarrow$ nm scale by using a surface modifier and their size effect on the fluorescence properties of europium doped yttria

Pramod K. Sharma\*, M.H. Jilavi, R. Nass, H. Schmidt

*Institut für Neue Materialien, Im Stadtwald, Geb. 43, D-66123 Saarbrücken, Germany*

Received 23 May 1997; received in revised form 27 March 1999; accepted 29 March 1999

---

## Abstract

The concept of tailored interfaces has been applied to the synthesis of  $\text{Eu}_2\text{O}_3/\text{Y}_2\text{O}_3$  powders to achieve a narrow size distribution by using a modifier. It was found that the particle size gradually decreased from  $6\ \mu\text{m}$  to  $10\ \text{nm}$  with an increase in concentration of the modifier from 0 to 10 wt% with respect to  $\text{Eu}_2\text{O}_3/\text{Y}_2\text{O}_3$ . Fluorescence spectra of the sample containing 10 wt% of surface modifier showed approximately a 5-fold enhancement of emission intensity of the  $^5\text{D}_0 \rightarrow ^7\text{F}_2$  transition of  $\text{Eu}^{3+}$ . This transition is the characteristic transition of europium for red fluorescence under UV light excitation. The concentration dependence of fluorescence in the range from 0–5 mol%  $\text{Eu}_2\text{O}_3$  did not reveal any concentration quenching.

*Keywords:* Nano size; Fluorescence; Yttria; Europium; Quantum particle

---

## 1. Introduction

It has been proven that the particles at the nanometer level have improved quality with respect to their potential application to various optical, electrical, mechanical and catalytic activity [1]. The particles, which range in size from a few, to several tens of nanometers, are called quasi-zero-dimensional mesoscopic systems, quantum dots, quantized or Q-particles [2]. Extensive research on

semiconductor quantum dots has shown that these particles have properties halfway between macroscopic (bulk) and microscopic (molecular like) substances and have recently aroused great interest in laser, photochemistry, and non linear optics [3–5]. Bawendi et al., have observed a number of discrete electronic transitions and a LO-phonon progression which were clearly resolved for the first time in a nanometer-scale cluster of CdSe [4]. Jungnickel and Henneberger have described the luminescence properties of semiconductor nanocrystals and the carrier processes that are relevant for the light emission [6]. Their study was concentrated on nanocrystals of  $\approx 5\ \text{nm}$  and hence observed strong carrier confinement. In the luminescence efficiency of ZnS:Mn nanocrystals, a size dependency has also been observed by Bhargava et al. [7]. They

---

\*Corresponding author. Present address: Center for Engineering of Electronics and Acoustic Materials, Pennsylvania State University, University Park, PA 16802, USA. Fax: +1-814-868-7967.

E-mail address: psharma@enr.psu.edu (P.K. Sharma)

stated that the  $Mn^{2+}$  ion d-electron states act as efficient luminescent centers while interacting with s-p electronic states of the host nanocrystal. They showed that this electronic interaction provides an effective energy transfer path and leads to high luminescent efficiencies at room temperature. It was concluded that nanocrystals doped with optically active luminescent centers may create new opportunities in the study and application of nanoscale materials.

In recent decades, luminescence properties of  $Eu^{3+}$  have attracted much attention as a dopant since they can emit red fluorescence with high luminescence efficiency under UV light excitation.  $Eu^{3+}$  behaves as activator center for scintillation and luminescence phenomena. These materials are important due to their direct application in cathodic picture tubes in color televisions and lasers. The requirements for these materials are high chemical purity, homogeneity, particle size in the nm-range, low production costs and high luminescence efficiency. It has motivated the basic research towards developing the materials that will efficiently luminesce. To enhance the europium emission intensity, many workers have activated it by codoping with either other rare earth or transition metal ions in different matrices [8]. Aspects such as, the effect of the crystal structure of the host material, the effect on clustering of  $Eu^{3+}$  by modifying the cation, the coordination environment of europium ion in glasses, and temperature have been studied extensively [9,10]. However, studies on the particle size dependent fluorescence behavior of  $Eu^{3+}$  doped yttrium oxide prepared by chemical solution route are scarce.

Chemical wet processes [11,12] are attractive means of synthesizing those materials since they offer a new level of control over the particle size, crystallinity and microstructure. This control is important from a materials engineering perspective since the performance of manufactured devices largely depends on these properties. The chemical growth control method is a suitable approach for preparing the fluorescence materials at a low temperature giving a high degree of homogeneity at the molecular scale with improved fluorescence properties of rare-earth-doped metal oxides [10].

Synthesis of a fine particulate system via a wet chemical method, requires control over the thermodynamics of the interfaces due to their tendency to minimize their surface energy by agglomerating or growing large particles. Use of a surface modifier in highly alkaline medium ( $pH > 10$ ) is one of the approaches to modify the surface of growing particles. During the coprecipitation of precursors the growth reaction can take place but growing together is prevented. In this work, we have synthesized  $Eu^{3+}$ -doped yttria by a chemically controlled method in the presence of surface modifiers which is a mixture of Tween-80 and Emulsogen-OG. Included is a detailed study on the control of particle size by altering the concentration of the modifier and the effect of particle size on the red fluorescence of  $Eu^{3+}$ . Also, a brief study on concentration dependent fluorescence from 0 to 5 mol% of  $Eu_2O_3$  will be presented.

## 2. Experimental

Solution (A) was prepared by dissolving 15.78 g (0.044 mol) of  $Y(NO_3)_3 \cdot 5H_2O$  and 0.590 g (3 mol%) of  $Eu(NO_3)_3 \cdot 5H_2O$  in ethanol. The solution was stirred for 2 h at room temperature. Another solution (B) was prepared by dissolving 10 wt% surface modifier (0.25 ml of tween-80 (polyoxyethylene(20)sorbitate; supplied by Aldrich) and emulsogen-OG (oelsauerepolyglycerinester; supplied by Hoechst) each) with respect to  $Eu_2O_3/Y_2O_3$  in 50 ml of an aqueous ammonium hydroxide solution ( $pH > 10$ ) and stirred for 1 h at room temperature. Solution (A) was then added to the modifier solution (B) drop by drop through a burette at a controlled rate (10 drops per minute) with vigorous stirring. The obtained gel was separated in a centrifuge at the rate of 6000 rpm for 30 min. The aqueous solution was removed by refluxing in toluene using a water trap, the toluene was removed by evaporation, and the resulting powder was dried in the oven at  $60^\circ C$  for 24 h. The final product was isolated as a white powder after heat treatment in a box furnace at  $450^\circ C$  for 2 h in ambient atmosphere.

The particle size of the powder was determined by a Microtrac particle size analyzer (UPA 9200).

Samples for particle size analysis were prepared by making a powder suspension in water. The suspension was then ultrasonicated for 15 min so the particles would not settle. The nanostructure determination of the particles was carried out on a high resolution transmission electron microscope (HRTEM) (Philips CM 200) operated at 200 kV with a line resolution of 1.4 Å. For the TEM specimen preparation, a copper grid which was covered with a very thin film of amorphous carbon was used. The copper grid was dipped in a suspension of the desired solution. The density of the powder was determined by a micrometrics densimeter (ACCUPYE 1330). A multipoint BET surface area determination was performed for all of the samples with a minimum of 5 points on the micrometrics unit (ASAP 2400). All powders were degassed at 150°C before surface area measurements. The thermal analysis (TG/DTA) was carried out in air on a Bähr Thermoanalyzer (STA 501) from room temperature to 800 °C. The infrared spectra of the samples were recorded on a Fourier transformation spectrometer (Bruker, IFS 25). The fluorescence spectra were measured with a Hitachi fluorescence spectrophotometer with a 150 W xenon lamp (3100).

### 3. Results and discussion

#### 3.1. Effect of modifier concentration on the particle size

Fig. 1 shows the variation in the particle size distribution versus the concentration of the modifier. A narrow size distribution is achieved when the powders were synthesized in the presence of the modifier. As the concentration of the modifier was increased from 0 to 10 wt% with respect to  $\text{Eu}_2\text{O}_3/\text{Y}_2\text{O}_3$ , the particle size was reduced from 6  $\mu\text{m}$  to 10 nm and the surface area increased from 4.45 to 34.87  $\text{m}^2/\text{g}$ . This enhancement in the surface area can be attributed to the decrease in particle size, as the surface area is inverse of particle's size [10]. The modifier protects the generated particles by forming a layer and reduces the surface free energy of the particulate matter to an appreciable extent which prevents interaction with neighboring particles. The size was consistent with that deter-

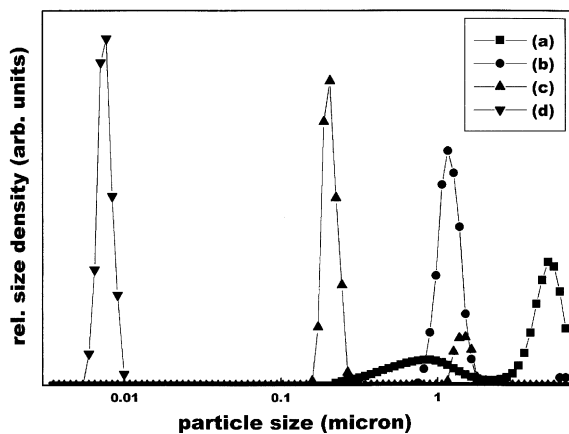


Fig. 1. Particle size distribution of powder containing modifier concentration in wt%: (a) 0, (b) 0.2, (c) 2.0 and (d) 10.

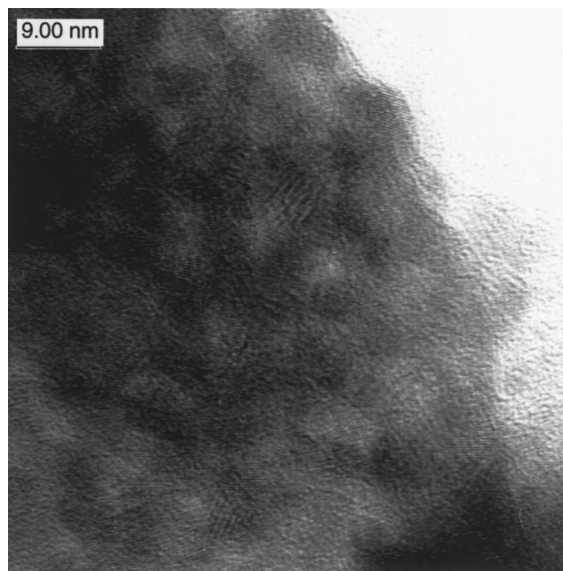


Fig. 2. HRTEM micrograph of europium doped yttria containing 10 wt% of modifier.

mined by a HRTEM study of the sample containing 10 wt% modifier (refer to Fig. 2). Lattice images of the particles help to distinguish the particles from each other for determining the particle size.

The modifier creates a surface modifier layer on the particles that can be maintained at  $\approx 350\text{--}380^\circ\text{C}$ . This is illustrated with the help of FTIR spectroscopy and TG/DTA study. Fig. 3

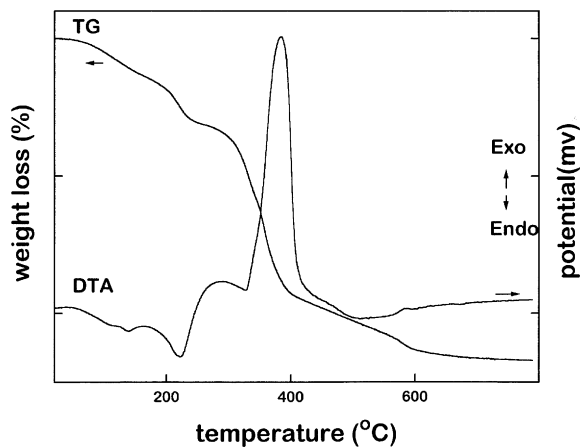


Fig. 3. TG/DTA curve of powder containing 10 wt% of modifier.

shows the TG/DTA curve for a sample in the presence of 10 wt% concentration of a modifier. The TG curve indicates the weight loss in three steps. The first weight loss was observed between 110°C and 180°C which can be assigned to the presence of adsorbed surface water. The second weight loss was attributed to dehydration of more strongly chemisorbed water which was noticed between 190°C and 210°C. The third weight loss in the temperature range from 300°C to 390°C was attributed to the removal of organic matter, e.g. solvent and organic modifier. These three weight loss steps were accompanied by two endothermic peaks (at 135°C and 200°C) and one exothermic peak (at 380°C) in the DTA curve. Similar DTA and TG trends were observed for 0.2 and 2 wt% modifier concentration. The exothermic peak at 330°C shifted to a higher temperature ( $\approx 380^\circ\text{C}$ ) with the

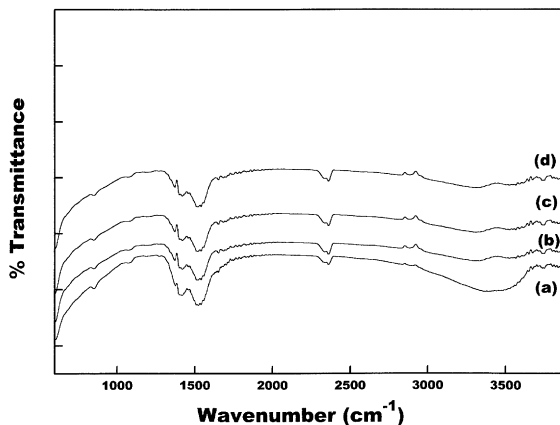


Fig. 4. FTIR spectra of powder containing modifier concentration in wt%: (a) 0, (b) 0.2, (c) 2.0 and (d) 10.

increase in concentration of modifier from 0 to 10 wt% (refer to Table 1). This shift can be attributed to the interaction of the modifier with the generated particles, which became stronger with the increased concentration of modifiers, and hence required a higher temperature for their removal [10,12,13]. This attribution is consistent with the infrared study (Fig. 4). The spectra were characterized by peaks between 1250 and 1800  $\text{cm}^{-1}$  which can be assigned to C-H, C-O, C-C bending, which were mainly due to organic matter [14,15]. The peak at 3300  $\text{cm}^{-1}$  is attributed to the O-H stretching vibration of metal hydroxide. No significant change was observed in the FTIR spectra of the powders derived at different concentrations of the modifier. Only the intensity of the peaks due to organic matter increased with the increase in the concentration of the modifier. As a consequence of this, the

Table 1  
DTA and surface area data of the powders synthesized under different modifier concentrations

Concentration of modifier (wt%)	Endothermic peak (°C)	Exothermic peak (°C)	Surface area ( $\text{m}^2/\text{g}$ )	Excitation wavelength (nm)
0	135,200	330	4.45	395
0.2	135,200	330	6.92	391
2.0	135,200	350	7.72	388
10.0	135,200	380	34.87	382

hydroxyl groups were removed before the surface modified layer was removed ( $\approx 380^\circ\text{C}$ ). Interparticle condensation was retarded and a uniform and narrow size distribution of the particles was obtained. This is consistent with our TG/DTA results.

### 3.2. Effect of particle size on $^5\text{D}_0 \rightarrow ^7\text{F}_2$ transition

A preliminary experiment was performed to optimize the excitation wavelength at which the maximum ions responsible for the  $^5\text{D}_0 \rightarrow ^7\text{F}_2$  transition (at region 614 nm) can be excited. The effect was most notable in the  $^5\text{D}_0 \rightarrow ^7\text{F}_1$  and  $^7\text{F}_2$  transition where the position of the higher-energy component depended significantly on the excitation wavelength. It was observed that the emission intensity of the  $^5\text{D}_0 \rightarrow ^7\text{F}_2$  transition was increased with an increase in excitation wavelength up to

394 nm. When the excitation wavelength increases from 394 to 404 nm, the emission intensity of  $^5\text{D}_0 \rightarrow ^7\text{F}_2$  decreased. Less significant variations in the  $^5\text{D}_0 \rightarrow ^7\text{F}_0$  and  $^7\text{F}_3$  transitions at 578 and 655 nm, respectively, were observed with the excitation wavelength [16]. Hereafter, all the fluorescence measurements were made at excitation wavelength of 394 nm.

The effect of particle size on the fluorescence behavior of the  $^5\text{D}_0 \rightarrow ^7\text{F}_2$  transition of  $\text{Eu}^{3+}$  in the yttria powder was found to be significantly higher as the concentration of the modifier increased (refer to Fig. 5). The most noteworthy feature of Fig. 5 is the sensitivity of the  $^5\text{D}_0 \rightarrow ^7\text{F}_2$  peak (614 nm) with the particle size. It was found that the peak emission intensity of the  $^5\text{D}_0 \rightarrow ^7\text{F}_2$  transition increases approximately five fold as the average particle size decreases from  $6\ \mu\text{m}$  to 10 nm. This suggests that

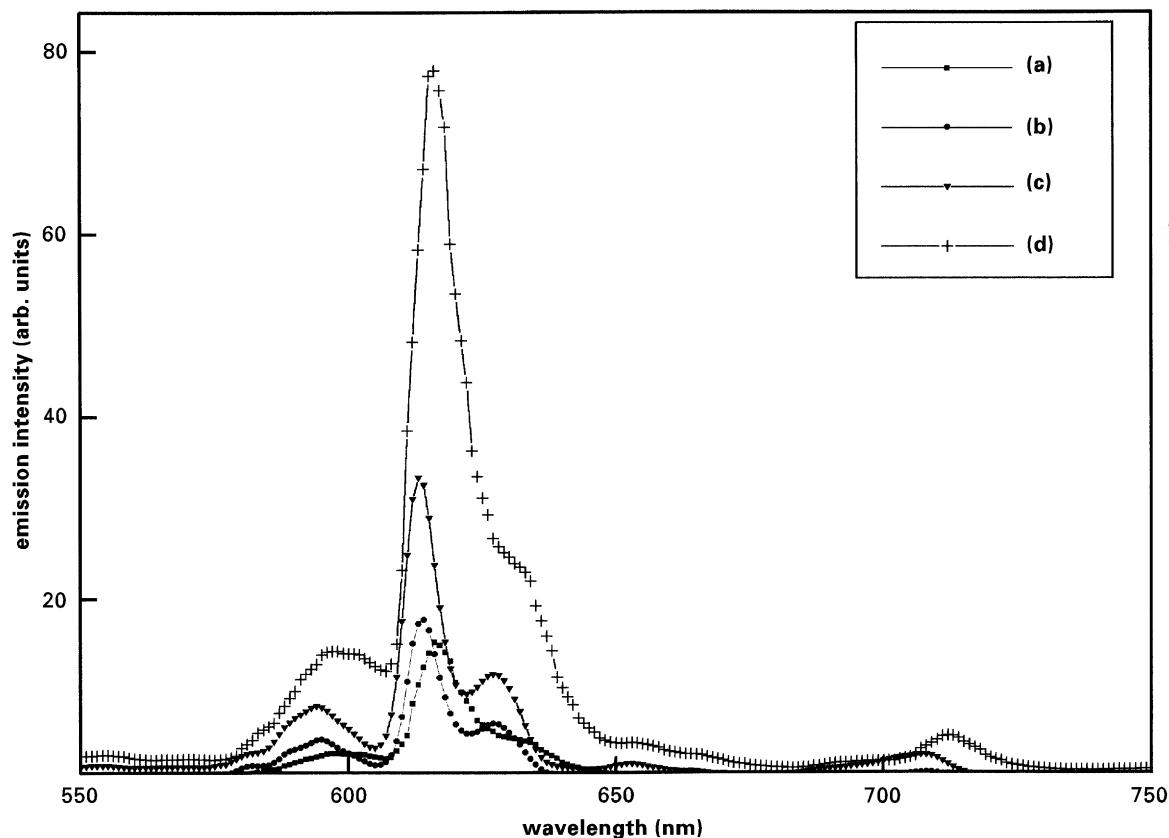


Fig. 5. Emission spectra of powder with the particle size: (a) 6, (b) 1, (c) 0.2 and (d) 0.01  $\mu\text{m}$ .

Table 2  
Effect of particle size on the energy of emission band

Particle size ( $\mu\text{m}$ )	$^5\text{D}_0 \rightarrow ^7\text{F}_1$ Peak position (FWHM) $\lambda$ (nm)	Energy of emission band (eV)	$^5\text{D}_0 \rightarrow ^7\text{F}_2$ Peak position (FWHM) $\lambda$ (nm)	Energy of emission band (eV)
6.0	596	2.080	616	2.012
1.0	594	2.087	616	2.016
0.2	594	2.087	614	2.019
0.01	595	2.084	616	2.012

the emission intensity of fluorescence varies inversely as the particle size increases. This behavior was expected from the quantum – confinement model as described by Bawendi et al. and Alivisatos et al. [4,5]. Goldburt et al. have observed a high luminescence efficiency in Tb-doped  $\text{Y}_2\text{O}_3$  nanocrystals which was measured at 18% as compared to 16% in the bulk [17]. They also stated that the nonradiative contribution decreased with a decrease in particle size. The size dependence of the fluorescence emission intensity can also be demonstrated in terms of the number of particles per unit area facing towards the incident light as described by Pramod et al. [10]. Increasing the surface area of smaller particles (refer to Table 1) leads to enhancement in the fluorescence intensity. Our study shows that, the particle size has a negligible effect on the energy of the  $\text{Eu}^{3+}$  emission band in the  $^5\text{D}_0 \rightarrow ^7\text{F}_1$  and  $^7\text{F}_2$  transition as indicated in Table 2. The wavelength was measured by full-width at half-maxima (FWHM) of the emission intensity peak for the determination of the energy of the emission band. Table 1 shows the effect of particle size on the wavelength which was extracted from comparable excitation spectra (not shown here) associated with the  $^7\text{F}_2 \rightarrow ^5\text{D}_0$  transition of the  $\text{Eu}^{3+}$  at the emission of 612 nm. All spectral features were found to be unchanged except for the intensity of the peak centered at 395 nm. The intensity of this peak increased with decreasing the particle size. On the other hand, the position of the peak shifted to lower wavelength (higher energy level) from 396 to 382 nm as the particle size decreased from 6 to 0.01  $\mu\text{m}$ . This shift in excitation spectra with

particle size is evidence of quantum confinement. It is consistent with the study of Gallagher et al. [13]. They have reported a shift of 60 nm (to shorter wavelength) in the excitation peak at the maximum emission from  $\text{Mn}^{2+}$ -doped ZnS nanocrystals with the decrease in particle size due to quantum confined ZnS.

### 3.3. Effect of fluorescing ion concentration on emission intensity of the $^5\text{D}_0$ to $^7\text{F}_1, ^7\text{F}_2$ transition

Fig. 6 shows the emission intensity of the  $^5\text{D}_0 \rightarrow ^7\text{F}_1$  and  $^7\text{F}_2$  transition of  $\text{Eu}^{3+}$  of calcined powder as a function of the europium concentration. It was stated that as the concentration of

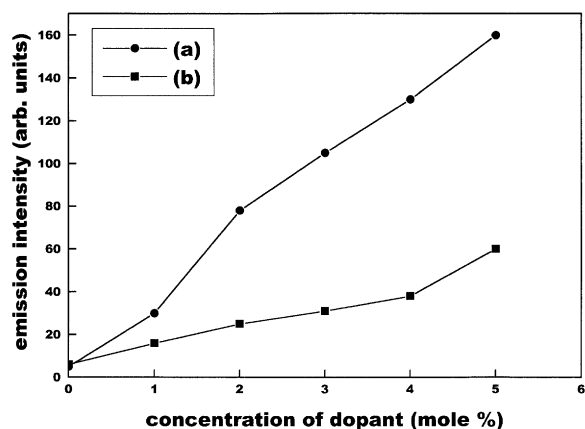


Fig. 6. Concentration dependence of emission intensity of (a)  $^5\text{D}_0 \rightarrow ^7\text{F}_2$  (614.5 nm) and (b)  $^5\text{D}_0 \rightarrow ^7\text{F}_1$  (587.6 nm) transitions at  $\lambda_{\text{ex}} \approx 394$  nm.

europium increased, the area under the fluorescent peaks of both the transitions increased. But the effect was more significantly observed in the  $^5D_0 \rightarrow ^7F_2$  transition of  $\text{Eu}^{3+}$ , although the peak positions of both transitions were found to remain unchanged for varying dopant concentration. It is suggested that there was no cross relaxation of neighboring  $\text{Eu}^{3+}$  which cause the transfer of energy from radiative to nonradiative europium centers. As Honma et al. stated, the concentration quenching is caused by the interaction between radiative and nonradiative  $\text{Eu}^{3+}$  [18]. Hence no concentration quenching was observed in the range 1–5 mol%. This result is consistent with the Arbuthnot et al. studies [19].

#### 4. Conclusions

This study indicates that the particle size and distribution can be controlled to a certain extent by alteration of the concentration of the emulsogen. Fluorescence properties of europium ion for the  $^5D_0 \rightarrow ^7F_2$  transition can be improved by controlling the particle size of europium doped yttria. To control the particle size, it is necessary to add a surface modifier that coats the surface of the particles and provides a barrier to agglomeration. The photoluminescence, which is sensitive to particle size, can be improved by reduction in particle size due to quantum confinement. The emission of the  $^5D_0 \rightarrow ^7F_2$  transition of  $\text{Eu}^{3+}$  was found to be more intensified with an increase in the concentration of europium. Therefore, no quenching effect was observed in the concentration range from 1 to 5 mol% of  $\text{Eu}^{3+}$ .

#### References

- [1] C.J. Brinker, G.W. Scherer, *Sol-gel Science: The Physics and Chemistry of Sol Gel Processing*, Academic Press, New York, 1990.
- [2] R.F. Khairutdinov, N.A. Rubtsora, S.M.B. Costa, *J. Lumin.* 68 (1996) 299.
- [3] A.A. Kortan, R. Hull, R.L. Opila, M.G. Bawendi, M.L. Steigerwald, P.J. Carroll, L.E. Bruce, *J. Am. Ceram. Soc.* 112 (1990) 1327.
- [4] M.G. Bawendi, W.L. Wilson, L. Rothberg, P.J. Carroll, T.M. Jedju, M.L. Steigerwald, L.E. Bruce, *Phys. Rev. Lett.* 65 (13) (1990) 1623.
- [5] A.P. Alivisatos, A.L. Harris, N.J. Lennox, Steigerwald, L.E. Bruce, *J. Chem. Phys.* 89 (7) (1988) 4001.
- [6] V. Jungnickel, F. Henneberger, *J. Lumin.* 70 (1996) 238.
- [7] R.N. Bhargava, D. Gallagher, X. Hong, A. Nurmikko, *Phys. Rev. Lett.* 72 (3) (1996) 416.
- [8] G. Chen, Y. Shi, B. Li, N. Zhang, Y. Chi, K. Dou, *J. Mater. Sci. Lett.* 14 (1995) 1707.
- [9] V.L. Costa, M.J. Lochhead, K.L. Bray, *Chem. Mater.* 8 (1996) 783.
- [10] Pramod K. Sharma, R. Nass, H. Schmidt, *Opt. Mater.* 10 (1998) 161.
- [11] Pramod K. Sharma, M.H. Jilavi, D. Burgard, R. Nass, H. Schmidt, *J. Am. Cer. Soc.* 81 (10) (1998) 2287.
- [12] Pramod K. Sharma, M.H. Jilavi, R. Nass, H. Schmidt, *J. Mater. Sci. Lett.* 17 (1998) 823.
- [13] D. Gallagher, W.E. Heady, J.M. Racz, R.N. Bhargava, *J. Mater. Res.* 10 (4) (1995) 870.
- [14] S. Doeuf, M. Henry, C. Sanchez, J. Livage, *J. Non-Cryst. Solids* 89 (1987) 20.
- [15] K. Nakamoto, *Infrared and Raman Spectra of Inorganic and Coordination Compounds*, 3rd Edition, Wiley, New York, 1978.
- [16] X.-P. Fan, M. Wang, G. Xiong, *J. Mater. Sci. Lett.* 12 (1993) 1552.
- [17] E.T. Goldburt, B. Kulkarni, R.N. Bhargava, J. Taylor, M. Liberta, *J. Lumin.* 72-74 (1997) 190.
- [18] T. Honma, K. Toda, Z. Ye, M. Sato, *J. Phys. Chem. Solids* 59 (8) (1998) 1187.
- [19] D. Arbuthnot, X.-J. Wang, E.T. Knobbe, *J. Non-Cryst. Solids* 178 (1994) 52.